# Single-shell carbon nanotubes of 1-nm diameter

## Sumio Iijima & Toshinari Ichihashi

Fundamental Research Laboratories, NEC Corporation, 34 Miyukigaoka, Tsukuba, Ibaraki 305, Japan

CARBON nanotubes[1] are expected to have a wide variety of interesting properties. Capillarity in open tubes has already been demonstrated[2-5], while predictions regarding their electronic structure[6-8] and mechanical strength[9] remain to be tested. To examine the properties of these structures, one needs tubes with well defined morphologies, length, thickness and a number of concentric shells; but the normal carbon-arc synthesis[10,11] yields a range of tube types. In particular, most calculations have been concerned with single-shell tubes, whereas the carbon-arc synthesis produces almost entirely multi-shell tubes. Here we report the synthesis of abundant single-shell tubes with diameters of about one nanometre. Whereas the multi-shell nanotubes are formed on the carbon cathode, these single-shell tubes grow in the gas phase. Electron diffraction from a single tube allows us to confirm the helical arrangement of carbon hexagons deduced previously for multi-shell tubes[1].

We found the single-shell tubules in soot-like deposits formed in a carbon-arc chamber similar to that used for fullerene production. Two vertical electrodes are installed in the centre of the chamber. The anode, which is the upper electrode, is a graphitic carbon rod 10 mm in diameter, and the cathode, a 20-mm-diameter carbon rod, has a shallow dimple used to hold a small piece of iron during evaporation. The evaporation chamber is filled with a gas mixture typically consisting of 10 torr methane and 40 torr argon. The carbon discharge arc was generated by running a d.c. current of 200 A at 20 V between the electrodes. The iron filings melted to form a droplet, and so generated iron vapour which cooled and condensed into small particles of iron carbide above the cathode. The vaporization of iron takes place simultaneously with the production of soot, both from methane and by evaporation from the carbon cathode. We noticed that no tubules were formed when the carbon arc reactor was operated with any one of the three components argon, iron and methane absent.

The catalytic role of iron is well known in carbon fibre production, in which iron particles are found on the fibre tips and act as heterogeneous deposition centres for carbon atoms from the vapour phase[12]. In the present experiment, we did not find iron particles at the tubule tips. We suspect, however, that atomic iron particles, presumably as a homogeneous catalyst in the vapour phase, somehow assist the formation of single-shell tubules. Specimens for electron microscopy were prepared from acetone suspensions of soot collected over the electrodes in the evaporation chamber. Nanotubes were placed on a microscope specimen grid by drying a drop of the suspension taken up on the grid. We used either an ultra-high-vacuum (JEM 200FXV) or conventional transmission electron microscope (Topcon 002B) at 120 kV or 200 kV accelerating voltage.

A typical electron micrograph showing a general view of the specimen is reproduced in Fig. 1a. Threads are curved and tangled together to form bundles in some regions. All the threads are found to be single-shell carbon nanotubes. Round, dark objects attached to the tubules are cementite ($Fe_3C$), as indicated by powder diffraction measurements and measurement of the $d$ spacings of lattice fringes (lattice images with spacings of around 0.2 nm were recorded on individual particles); these particles range in size from a few nanometres to several tens of nanometres, which were mostly coated with a few graphite layers. Some of the particles were soluble in nitric acid.

The nanotubes often form as bundles, but isolated and single tubules are also present. Three tubules which bridge two cementite particle agglomerates are seen in Fig. 1b. On the upper right-hand side, a graphitic layer showing an image of the basal plane with lattice spacing 0.34 nm can be recognized. From this, we calibrated the magnifications of the tubules. All micrographs were recorded at optimum focus[13], so that two dark lines in the tubule image correspond to side portions of the cylinders. The thinnest tube in this micrograph (labelled 1) is 0.75 nm in diameter, and is attached to a thicker (13-nm) tube (labelled 2). Tubules 1 and 2 are slightly curved, but tubule 3 (diameter 0.92 nm) spans straight across a 140-nm opening between two cementite particle agglomerates. The longest single-shell tubule was 700 nm long with a diameter of 0.9 nm.

Short and terminated tubules are commonly observed (4 and 5 in Fig. 1b). The terminated tubule labelled 6 moved gradually during the observation so that one end appears to be fading out. No cementite particles were found on the free tips of the tubules, but they are entangled with cementite particle agglomerates. The tubules are capped in shapes that have been reported previously[14,15] (arrow 4 in Fig. 2).

We carefully measured the diameters on the electron micrographs of individual tubules. Figure 2 shows a histogram of the diameters of about 60 tubules, which range from about 0.7 nm to 1.6 nm. Two peaks are seen at tubule diameters of around 0.8 nm and 1.05 nm; we believe that these peaks are significant. The origin of the preferred tubule diameters is interesting to consider in terms of the tubule helicity and growth.

Figure 3a shows an electron diffraction pattern taken from a 1.37-nm single-shell tubule together with its corresponding



FIG. 1a, Electron micrograph showing bundles of single-shell carbon nanotubes which are curved and entangled. Dark blobs are cementite particles which assist in tubule growth. A terminated tubule is indicated by an arrow. b, Electron micrograph showing individual single-shell nanotubes. The tubule labelled 1 is 0.75 nm in diameter and tubule 2 is 1.37 nm in diameter. A straight tubule (3) and two terminated ones (4 and 5) can also be seen.
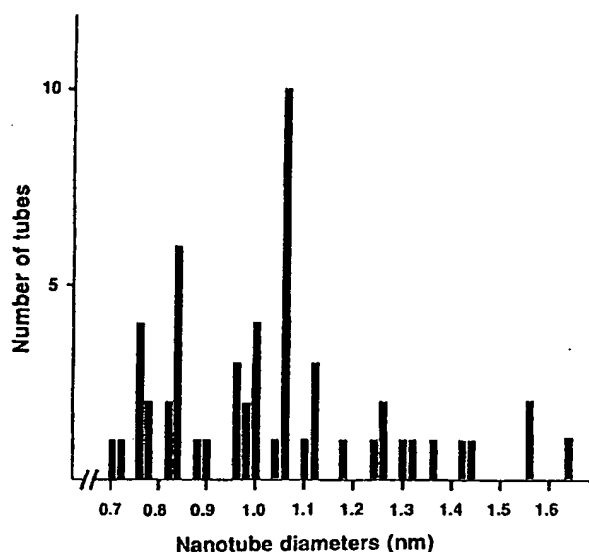
FIG. 2 Histogram showing frequency of single-shell nanotubes of different tubule diameters. Two peaks, at 0.8 nm and 1.35 nm, are dominant.

electron micrograph (Fig. 3b). The tubule is attached to the bundle of tubules seen at the left-hand side. An electron beam (20 nm diameter) was focused on to the tubule, so that the area diffracting the electrons comprised about 2,000 carbon atoms. This small scattering volume and the cylindrical structure are responsible for the extremely weak and diffused diffraction intensities. There are two hexagonal ($hk0$) diffraction patterns rotated $\pm \alpha/2$ from perfect alignment along the tube axis, and these patterns show mirror symmetry both along and perpendicular to the tube axis. The mirror symmetry confirms helicity in the single-shell tubule structure, as was found previously for

multi-shell tubules[1]. All electron diffraction patterns observed in the present sample showed the $2mm$ symmetry. The ($00l$) spots coming from the graphite basal lattice plane, which were observed for the multi-shell tubes, are completely absent (see Fig. 3 of ref. 1).

The spots are streaked vertically because of the fibrous structure. Each streaked spot in Fig. 3a has intensity maxima appearing with a period (indicated by triple arrows) of 0.73 nm$^{-1}$. The value corresponds to the diameter measured on the tubule (1.37 nm). The modulation can be explained by Fraunhofer diffraction from two vertical portions of the tubule
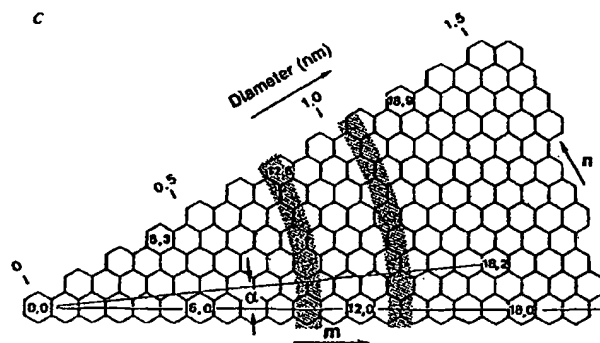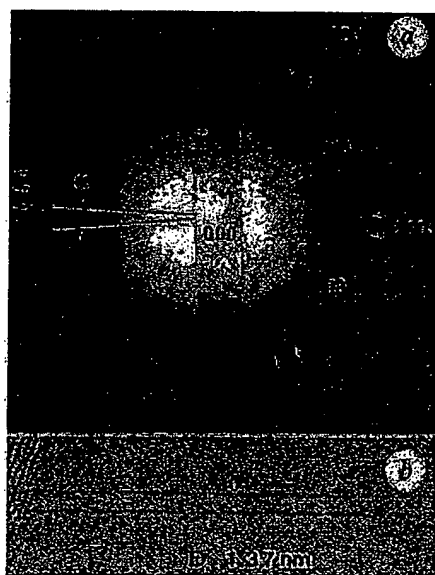




FIG. 3a, Electron diffraction pattern taken from a single-shell nanotubule of diameter 1.37 nm. b, Electron micrograph of same tubule. The pattern comprises two sets of the hexagonal patterns which gives rise to splitting of the ($hk0$) spots. Each spot has periodic intensity maxima in the vertical direction, caused by Fraunhofer diffraction from the two portions of the tube imaged as two dark lines in b. c, Schematic representation of helical tubules according to Hamada's notation[6]. A tubule is represented by an index ($m$, $n$) or ($m$, $\alpha$), where $m$ is $m$th hexagon from the origin (0, 0), and $n$ and $\alpha$ are defined as shown. $\alpha$ is a pitch angle. If the tubule diameter $D$ and angle $\alpha$ are known, the tubule structure is uniquely determined. Hatched hexagons represent the tubules corresponding to the two peaks in Fig. 2.

parallel to the incident electron waves.

By knowing the tubule diameter $D$ and its pitch angle $\alpha$ with respect to the fibre axis (Fig. 3a), the helicity and thus the tubule structure can be determined uniquely. To describe the tubule helicity, we follow Hamada's notation[6] as illustrated in Fig. 3c, where a tubule can be represented by an index $(m, n)$. This tubule can be realized by rolling up a sheet of hexagons so as to superimpose the origin $(0, 0)$ on the hexagon $(m, n)$. A tubule $(m, -n)$ is chiral with the opposite handedness to $(m, n)$, and thus they should be optically active, but they cannot be distinguished by the diffraction experiment. The tubules which were observed frequently on the histogram (Fig. 2) have values of $(m, n)$ in the hatched areas. On the electron diffraction pattern in Fig. 3a, $\alpha$ and $D$ are measured as $7°$ and 1.37 nm, respectively. This tube can be indexed as (18, 2) or its

enantiomer (18, −2), and should behave as a semiconductor according to electronic band structure calculations[6,16]. We should mention here that $\alpha$, or helicity, varies for a given tubule diameter.

We speculate that the single-shell tubules might be the embryo for the multi-shell tubules. In our proposed model for the nanotube growth[17,18], the tubule ends are open so that carbon atoms are easily captured at dangling bonds, and the multi-shell tubules grow in the direction of the tube axis and also perpendicular to it. The latter growth is associated with layer-by-layer growth on the tubule surface. In the single-shell tubes, we assume that axial growth dominates over layer growth. We speculate that the iron in the present experiments acts as a homogeneous catalyst in the vapour phase.  □

1. Iijima, S. Nature 354, 56–58 (1991).
2. Ajayan, P. M. & Iijima, S. Nature 361, 333–334 (1993).
3. Ajayan, P. M. et al. Nature 382, 522–523 (1993).
4. Tsang, S. C., Harris, P. J. F. & Green, M. L. Nature 362, 520–522 (1993).
5. Pederson, M. R. & Broughton, J. O. Phys. Rev. Lett., 69, 2687–2692 (1992).
6. Hamada, N., Sawada, S. & Oshiyama, S. Phys. Rev. Lett. 68, 1579–1581 (1992).
7. Mintmire, J. W., Dunlap, B. I. & White, C. T. Phys. Rev. Lett. 68, 631–634 (1992).
8. Saito, R., Fujita, F., Dresselhaus, G. & Dresselhaus, M. S. Phys. Rev. B 46, 1804–1811 (1992).
9. Robertson, D. H., Brenner, D. W. & Mintmire, J. W. Phys. Rev. B 45, 12592–12595 (1992).
10. Ebbesen, T. W. & Ajayan, P. M. Nature 368, 220–222 (1992).
11. Ando, Y. & Iijima, S. Jpn. J. appl. Phys. 32, L107–L109 (1993).
12. Oberlin, A. & Endo, M. J. Cryst. Growth 32, 335–349 (1976).
13. Iijima, S. Chem. Scripta 14, 117–123 (1978–79).
14. Iijima, S., Ichihashi, T. & Ando, Y. Nature 356, 776–778 (1992).
15. Ajayan, P. M. Ichihashi, T. & Iijima, S. Chem. Phys. Lett. 202, 384–388 (1992).
16. White, C. T., Robertson, D. H. & Mintmire, J. W. Phys. Rev. B 47, 5485–5488 (1993).
17. Iijima, S., Ajayan, P. M. & Ichihashi, T. Phys. Rev. Lett. 69, 3100–3103 (1992).
18. Iijima, S. Mat. Sci. Enging B. (in the press).

# Cobalt-catalysed growth of carbon nanotubes with single-atomic-layer walls

**D. S. Bethune, C. H. Klang\*, M. S. de Vries, G. Gorman, R. Savoy, J. Vazquez & R. Beyers**

IBM Research Division, Almaden Research Center, 650 Harry Road, San Jose, California 95120-6099, USA

CARBON exhibits a unique ability to form a wide range of structures. In an inert atmosphere it condenses to form hollow, spheroidal fullerenes[1–4]. Carbon deposited on the hot tip of the cathode of the arc-discharge apparatus used for bulk fullerene synthesis will form nested graphitic tubes and polyhedral particles[5–8]. Electron irradiation of these nanotubes and polyhedra transforms them into nearly spherical carbon 'onions'[9]. We now report that covaporizing carbon and cobalt in an arc generator leads to the formation of carbon nanotubes which all have very small diameters (about 1.2 nm) and walls only a single atomic layer thick. The tubes form a web-like deposit woven through the fullerene-containing soot, giving it a rubbery texture. The uniformity and single-layer structure of these nanotubes should make it possible to test their properties against theoretical predictions[10–13].

The initial aim of our experiments was to produce metallofullerenes and graphite-encapsulated nanocrystals of magnetic atoms. Electrodes were prepared by boring 4-mm-diameter holes in 6-mm-diameter graphite rods and filling them with mixtures of pure powdered metals (Fe, Ni or Co) and graphite. These filled anodes (~ 2 at % metal) were vaporized with a current of 95–105 A in 100–500 torr of He in our arc fullerene generator. The results obtained with cobalt were unique.

When a Co-containing rod was used, what looked like spider webs formed in the chamber, draping between surfaces. The soot on the chamber walls was rubbery and could be peeled off in long strips. Normal fullerene soots (and those made with Fe- or

Ni-containing rods) are crumbly. The soot and the web material were ferromagnetic. A transmission electron microscope (TEM) image of the web material (Fig. 1) shows that the web consists of rounded soot particles a few nanometres across, linked together by fine fibres. Individual threads can be traced for several micrometres. In some cases several fibres converge on a soot particle. Embedded within the soot particles are round cobalt clusters with diameters ranging from a few nanometres to roughly 20 nm. Both electron and X-ray diffrac-
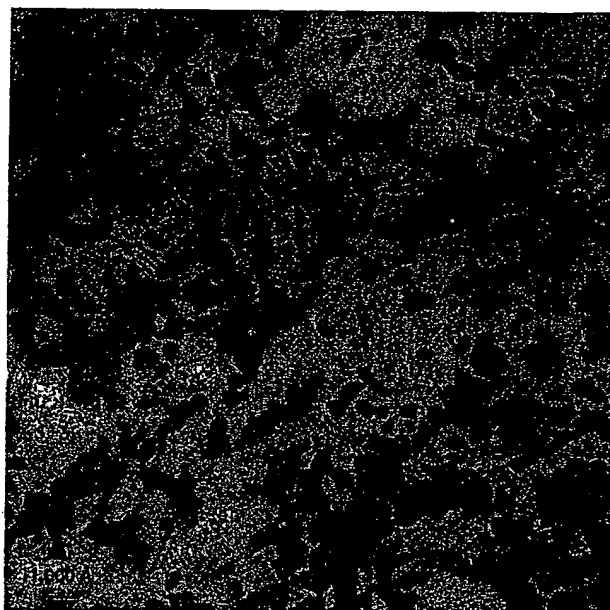


FIG. 1 Transmission electron micrograph of web-like material showing strands of thread-like fibres and cobalt clusters (dark spots) embedded in carbon soot particles. This image and those in Figs 2 and 3 were obtained using a Topcon 002B microscope operating at 200 kV and a Gatan Model 679 slow-scan camera to acquire digital images, which can then have the contrast enhanced to reveal the nanotubes.

**605**